
Growth, crystal structure, thermal properties and optical anisotropy of Tl_4CdI_6 single crystals [*]

[1]Franiv A. V., [1]Kushnir O. S., [2]Girnyk I. S., [3]Franiv V. A., [4]Kityk I.,
[5]Piasecki M. and [6]Plucinski K. J.

[1] Electronics Faculty, Ivan Franko Lviv National University, 107 Tarnavski St., 79017 Lviv, Ukraine, e-mail: o_kushnir@franko.lviv.ua
[2] Scientific, Technical and Educational Centre of Low-Temperature Studies at Ivan Franko Lviv National University, 50 Dragomanov St., 79005 Lviv, Ukraine
[3] Physics Faculty, Ivan Franko Lviv National University, 8 Kyrylo and Mefodiy St., 79005 Lviv, Ukraine
[4] Electrical Engineering Department, Czestochowa University of Technology, ul. Armii Krajowej 17, Czestochowa, Poland, e-mail: i.kityk@wsp.czest.pl
[5] Institute of Physics, Jan Dlugosz University Czestochowa, ul. Armii Krajowej 13/15, Czestochowa, Poland, e-mail: m.piasecki@ajd.czest.pl
[6] Electronics Department, Military University of Technology, ul. Kaliskiego 2, Warsaw, Poland

Received: 17.11.2012

Abstract. We report on the growth and initial thermal and optical characterisation of a single-crystalline ternary halide, Tl_4CdI_6. The crystal is described by the centrosymmetric tetragonal class *P*4/*mnc* at the room temperature. The parameters of linear thermal expansion are studied in the temperature region 330–500 K. The crystal is optically positive and reveals very high optical anisotropy (the birefringence ~ 0.13 at 633 nm). Its optical pseudo-gap value corresponds to wide-gap semiconductors. A broad maximum at 400–410 K found in the temperature dependence of IR radiation-induced second harmonic generation may be indication of a polymorphic phase transformation.

Keywords: ternary halide crystals, A_4BX_6, thermal expansion, inversion centre, optical anisotropy, second harmonic generation, phase transformations

PACS: 42.65.Ky, 61.10.Nz, 61.66.Fn, 64.70.Kb, 65.70.+y, 78.20.Fm
UDC: 548.0, 535.5

1. Introduction

In recent years one can see an upsurge in the interest of researchers in semiconductor ternary halides such as Tl_4HgI_6, Tl_4CdI_6, In_4CdI_6, Tl_4PbI_6, etc. They represent a large group of A_4BX_6 compounds (with A = In, Tl, ..., B = Mg, Zn, Cd, Hg, Ge, Pb, ..., and X = Cl, Br, I), which should be iso-structural or, at least, reveal very similar structures (see [1]). The attention is caused by a number of factors. Many ternary halides, e.g. Tl_4HgI_6, reveal attractive conductivity properties and represent heavy-metal (e.g., thallium) solid-state ionic conductors [2–5]. This also arouses interest in their application for chemical sensors [6]. The above crystals are also being extensively examined as bright and ultra-fast scintillating materials for medical imaging, high-energy and nuclear physics [7, 8].

---

[*] The materials of this work have been reported at the 2nd Ukrainian–Polish–Lithuanian Meeting on Ferroelectrics Physics (9–13 September 2012, Lviv, Ukraine).

High optical transmittance of the ternary halides, which can sometimes reach as far as up to 30–50 μm, makes them promising materials for the long-wavelength IR range and, in particular, for the far-IR nonlinear optics (see [9–11]). However, as shown by many earlier studies (see, e.g., [12–14]), the compounds of the A_4BX_6 family crystallise in a centrosymmetric point symmetry group 4/*mmm*, which hinders nonlinear optical applications and requires additional measures such as, e.g, periodic poling [10, 11]. In this respect it is also important that there has been a controversy concerning the availability of inversion centre in the most thoroughly investigated compound Tl_4HgI_6, and the authors of the works [15, 16] have stated that it is described by the acentric group 4*mm*. Another point of dispute is availability of phase transformations related to ionic conductivity and thermo-chromic effect in the ternary halides (see, e.g., [3, 4, 17, 18]).

As follows from the said above, it would be interesting to study the effect of synthesis and growth conditions on the structural features, thermal and anisotropic properties of the ternary halides Tl_4HgI_6 and Tl_4CdI_6. Since the former compound is relatively better investigated and some of the appropriate results have been reported in our recent work [19], the aim of the present work is to study the structure, thermal expansion, and the optical anisotropy of Tl_4CdI_6, in order to get more information on the prospects of the latter crystal concerned with nonlinear optics.

2. Experimental techniques

2.1. Synthesis and crystal growth

In order to synthesise thallium cadmium iodide, we used commercially produced salts of the relevant metal halides. The initial components were taken according to equi-molar ratios. Preliminary purification of the salts was performed using reiterated (up to 20 zones) re-crystallisation from the melt in quartz ampoules, and a vacuum sublimation.

Tl_4CdI_6 single crystals were grown with a standard Bridgman–Stockburger technique, using quartz ampoules with a conical bottom and the diameter of 12 mm. The ampoule containing a mixture of purified starting halides of a needed molar content was evacuated down to the pressure of 10^{-5} mm Hg for 3 h and simultaneously heated up to the temperatures $T = 470 - 570$ K (notice that the melting temperature is equal to ~ 670 K). After that the ampoules were annealed and placed into growing furnace. During the growing process, the ampoule was pulled down through the crystallisation zone with the rate of 0.5 mm/h. The temperature in the upper part of the furnace was set to be about 50 K higher than the melting point of the substance.

The necessary conditions of this growing technique were stability of the temperature and the rate of displacement of the ampoule, along with a plane front of crystallisation. The latter factor represented a demand crucial for growing high-quality single crystals, since it was just radial temperature gradients that would impose internal mechanical stresses, dislocations of relatively high densities, and appearing of polycrystalline features. An optimal crystallisation regime corresponded to the condition when the growth rate was exactly equal to the displacement rate of the ampoule through the crystallisation zone. In connection with this demand, we empirically chose the best temperature gradient and the ampoule displacement rate values.

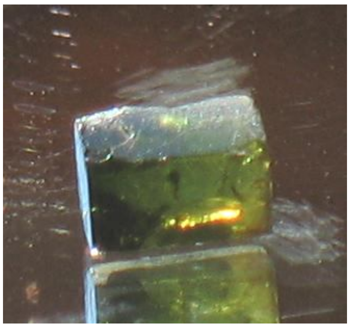

Fig. 1. Appearance of Tl_4CdI_6 single crystals grown with a Bridgman–Stockburger technique.

The temperature of a heater was kept constant with the aid of an electronic controlling scheme, which ensured the temperature stability of ±1 K inside the crystal growth zone. After completing the growth procedure, the temperature of the furnace was lowered down to 420 K and the crystal was annealed for 24 h. In this way we obtained Tl_4CdI_6 single crystals of fairly good optical quality, with the diameter of 12 mm and the typical length of 15 mm (see Fig. 1).

2.2. Crystal structure

Prior to X-ray structural studies, we prepared powder samples while grinding carefully the initial massive single-crystalline samples in an agate pounder. A uniform layer of the sample powder was coated on a special film prepared for the X-ray transmission experiments using an 'X-ray amorphous' glue. Then the powder was fixed with another film inside an X-ray transmittance cell.

Arrays of experimental intensities and reflecting angles were derived using an automated diffractometer STOE STADI P (producer STOE&Cie GmbH, Germany). A modified Guinier geometry was used, with the other typical characteristics and specifications described as follows: Cu $K\alpha 1$-irradiation ($U = 40$ kV and $I = 37$ mA), linear position-sensitive detector PSD, a curved Ge (111) monochromator of a Johann type, a $2\theta/\omega$ scanning regime, the angular 2θ interval $6.000 \le 2\theta \le 108.225°$ (with the angular step 0.015° 2θ), the step 0.480° 2θ of the detector, the time interval of 120–250 s for scanning a single angular step, and the working temperature $T = 297.0 \pm 0.5$ K.

Experimental linear extinction coefficients were determined using a logarithmic intensity ratio for the initial beam and the beam transmitted through background and working samples. The apparatus was certified using known standards NIST SRM 640b (Si) and NIST SRM 676 (Al_2O_3) [20]. Primary processing of the experimental data, calculations of theoretical diffractograms and indexing of the unit cell were performed with STOE WinX^{POW} (Version 2.21) software [21].

2.3. Thermal expansion and optical experiments

Thin (~ 0.5–2.0 mm) plates of Tl_4CdI_6 were prepared for our experiments using standard methods for treatment of our initial single-crystalline samples. The *c* axis was oriented in the plane of plate faces or perpendicular to it. The plates were preliminarily checked for optical homogeneity and residual mechanical strains, using conoscopic patterns observed with a polarising microscope MIN-8.

The relative linear thermal expansion $\Delta L / L$ along the *c* axis as a function of temperature was measured with a computer-controlled quartz dilatometer having a capacitive sensitive element (the thickness sensitivity of 1–2 nm – see, e.g., [22]). The temperature of samples in the region ~ 330–500 K was controlled using a thermostat with the accuracy of about 0.05–0.1 K. Variations of the temperature corresponded to regimes of continuous heating or cooling, with a typical temperature change rate $\mathrm{d}T/\mathrm{d}t \approx 50$ K/h. The linear thermal expansion coefficient was calculated on the basis of formula $\alpha = L^{-1}\dfrac{\mathrm{d}\Delta L}{\mathrm{d}T}$ with the aid of numerical differentiation. No preliminary smoothing of the raw data set $\Delta L / L(T)$ was performed.

Keeping in mind large refractive indices typical for the ternary halides, we studied the refractive indices for the ordinary (*o*) and extraordinary (*e*) rays in Tl_4CdI_6 (the polarisations of electric component $E \perp c$ or $E \parallel c$, respectively), using a laser ellipsometer LEF-3M (the light wavelength $\lambda = 633$ nm). We ensured that only eigenwave light polarisations were excited under varying experimental conditions of our ellipsometric experiments, in order to deal only with diagonal reflection matrix components. High-quality Glan–Thompson prisms were employed as polarisers when studying anisotropy of refractive properties of our crystals.

To examine optical transmittance in the vicinity of fundamental absorption edge and the relevant differences for the ordinary and extraordinary waves, we used a double-grating spectral luminescent complex SDL-1. The experiments were performed at the room temperature ($T = 297$ K) for both the ordinary and extraordinary polarisations of light in the photon energy region of 1.75–2.95 eV. The corresponding spectra were corrected at one-surface reflectance R while comparing the light intensity data obtained for the reference and working channels. In other words, we measured in fact the quantity $J/(1-R)^2$, with J being the experimental transmittance.

According to a standard technique, a second harmonic generation (SHG) with no phase matching was studied at the fundamental wavelength of 5.5 μm, using a basic CO_2 laser with the pulse duration 2 μs. Following from preliminary information about a possible inversion symmetry of Tl_4CdI_6, we also studied the SHG signal occurring after the crystal is photo-treated (see [23]). The reason is that optical irradiation can induce dc electric fields in a crystalline medium, which have acentric nature and so break down the inversion symmetry of a crystal and make possible observing second-order nonlinear effects, even if the crystal indeed were initially centrosymmetric. In other words, the effect of photo-stimulated second harmonic generation is symmetry-allowed.

The fundamental beam was split into two and one of them was preliminarily doubled in frequency (the wavelength of 2.75 μm; Ag_3AsSe_3 crystal). These focused beams irradiated our sample for several minutes (the other details of these standard experiments might be found, e.g., in Refs. [24, 25]). Polarisations of both the fundamental and doubled-frequency beams corresponded approximately to the geometry $E \perp c$. Then the doubled-frequency beam was turned off, the crystal was irradiated only by the light of fundamental frequency, which propagated approximately along the c axis, and the relative intensity of the photo-induced SHG in Tl_4HgI_6 was detected after 3–4 min of the bicolour treatment. When measuring a temperature dependence of the SHG effect, we placed the sample into a thermostat with ZnSe windows transparent in the IR range. In the same way as in the case of thermal expansion, both cooling and heating regimes were studied.

3. Results and discussion

Fig. 2 shows the experimental powder diffractograms of Tl_4CdI_6. The crystalline structure identified by us is tetragonal, being described by the spatial symmetry class $P4/mnc$. The calculated cell parameters are $a = b = 9.222$ Å and $c = 9.603$ Å ($\alpha = \beta = \gamma = 90°$), with two formula units per cell (Z = 2). The density is equal to $\rho = 6.88$ g/cm^3 and the unit cell volume is 816.69 Å^3. It is worthwhile that our cell parameters agree perfectly with those found in the study by Beck and Milius [13] and are only $(2–3)\times10^{-2}$ per cent different from the figures reported earlier by Zandberger [1]. The conclusion about the inversion symmetry of Tl_4CdI_6 is also in accordance with the results of those studies. However, this does not conform to the findings of the works [15, 16] concerning the acentric group $P4_2bc$ for the isomorphous Tl_4HgI_6 compound.

It cannot be excluded completely that the contradiction between the results of different authors for the spatial symmetry of ternary halides are due to experimental errors of some kind. On the other hand, it is quite probable that even subtle changes in the synthesis and/or growth conditions can influence the structural properties. In this respect the results [16, 18], which give the relevant examples, seem to be clarifying. In particular, we can admit that the centrosymmetric structure can appear as a result of 'racemisation' of polar substructures with the opposite polarity signs (see [16]), although the exact conditions of this 'racemisation' formulated in [16] do not seem to correspond to our growth conditions.

The temperature dependences of the parameters $\Delta L/L$ and α of linear thermal expansion along the c axis measured in the heating run are depicted in Fig. 3. As seen from Fig. 3a, the rate of thermal expansion gradually slows down with increasing temperature, which corresponds to decrease in the coefficient α at high temperatures. Since the linear and polynomial (the order $n = 2$ or 3) fits of the curve $\alpha(T)$ are almost of the same goodness, one can restrict analytical description of the temperature dependence of expansion coefficient to a simplest linear function ($\alpha(T) = a + bT$, with the coefficients $a = 1.448\times10^{-4}$ K^{-1} and $b = -2.931\times10^{-7}$ K^{-2}). Notice that the experimental noise in Fig. 3b which is more pronounced for lower temperatures is associated with a finite accuracy of temperature control.

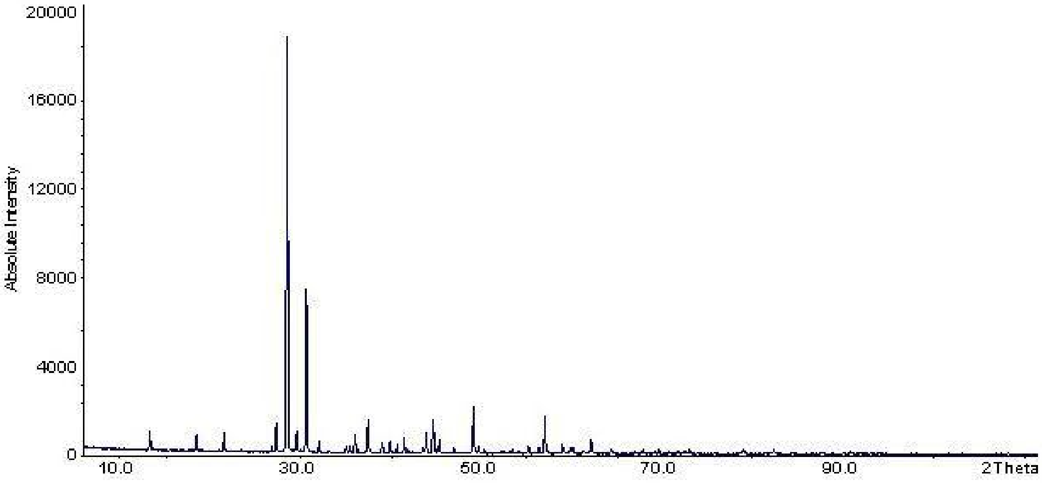

Fig. 2. Room-temperature diffractogram of Tl_4CdI_6 crystals (see text).

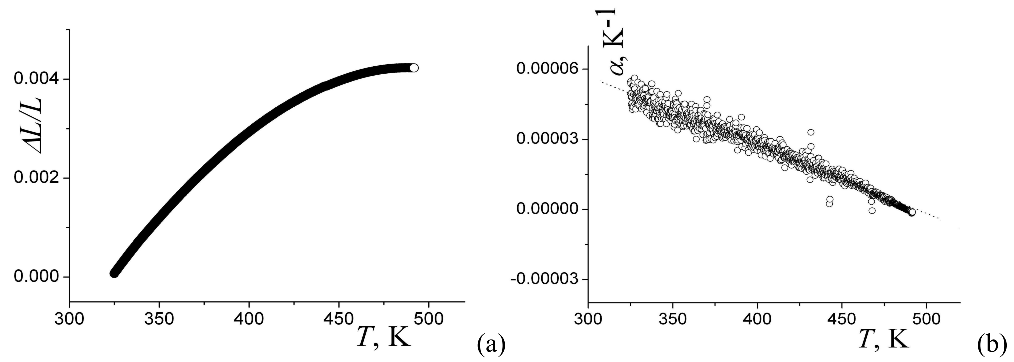

Fig. 3. Relative linear thermal expansion $\Delta L/L$ (a) and thermal expansion coefficient α (b) along the *c* axis obtained for Tl_4CdI_6 crystals in the heating run. Dotted line in panel (b) displays a simplest linear fit.

Against such a strong background, no clear evidence of structural transformations is seen. This does not confirm the results of the study [4] where a phase transition has been detected at about 403 K, issuing from the temperature behaviours of the conductivity and the dielectric permittivity (see also further discussion). We remind in this respect that the thermal expansion of the isomorphous Tl_4HgI_6 crystals behaves quite differently and reveals distinct anomalies observed in the same temperature region (410 and 450 K respectively in the cooling and heating runs – see [19]), which have been ascribed to the phase transitions. Moreover, we have obtained no clear differences between the heating and cooling runs, which might have evidenced a hysteresis.

Having clarified the thermal properties of Tl_4CdI_6, we proceed to their main optical characteristics. As seen from Fig. 4a, the optical transmittance of our crystals begins to fall down rapidly with approaching the region of blue visible light. Using common methods, one obtains the optical pseudo-gap values $E_{g\|} = 2.725$ eV and $E_{g\perp} = 2.638$ eV corresponding to the polarisations of the ordinary ($E \perp c$) and extraordinary ($E \| c$) rays. A relevant anisotropy parameter equal to $\Delta E_g = 87$ meV has to be regarded as large enough, thus resulting in significant anisotropy of the other optical characteristics.

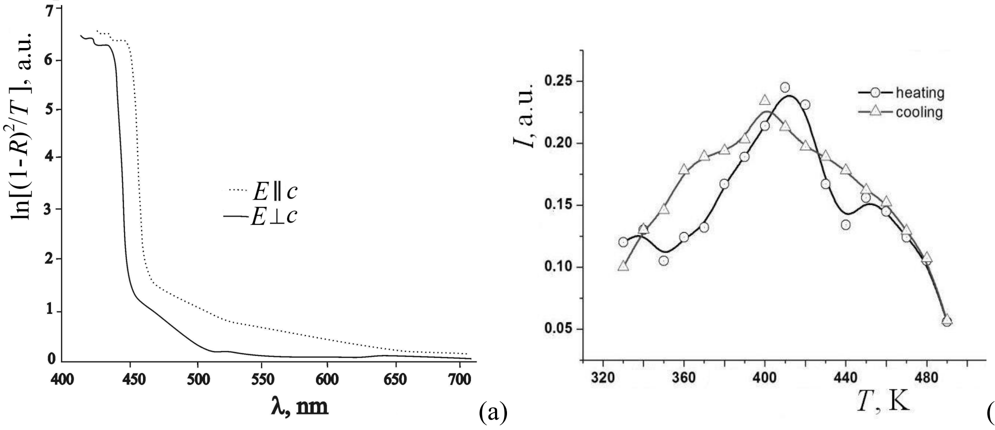

(a) (b)

Fig. 4. Temperature dependences of parameter $J/(1-R)^2$ describing optical absorbance near the fundamental absorption edge measured at the room temperature (a) and relative intensity I of photo-induced SHG (b) for Tl_4CdI_6 crystals. Solid lines in panel (b) are only for the guide of eye.

The refractive indices determined at the visible He-Ne laser wavelength of 633 nm are $n_o = 2.476$ and $n_e = 2.344$. Tl_4CdI_6 crystals turn out to be optically negative and the magnitude Δn of their optical birefringence equals approximately to 0.132. Notice that Tl_4HgI_6 crystals turn out to be optically positive ($n_o = 2.217$, $n_e = 2.386$ and $\Delta n = 0.169$). This dissimilarity agrees with structural differences of the above compounds (we have $c < a$ for Tl_4HgI_6 [19] and $c > a$ for Tl_4CdI_6). Despite the parameter c/a defining tetragonal distortion of a virtual cubic structure in the Tl_4CdI_6 crystals is not so large ($c/a = 1.04$), the optical anisotropy represented by the birefringence is very high. A comparison with, e.g., lead germanate crystals [26] having fairly similar absorption characteristics, testifies almost 4 times as large Δn value for Tl_4CdI_6. This birefringence is of the order typical for TeO_2, $TlGaSe_2$ and $CaCO_3$ crystals (see [26]), though at the price of worse optical transparency of Tl_4CdI_6 in the visible range, when compare to the latter compound.

Our experiments have indicated that the SHG signal is too small to be detected against the background of experimental noise. In other words, the crystals under test should be considered as revealing no SHG effect. This agrees with the obvious fact that direct observations of second-order nonlinear optical effects described by a third-rank polar tensor are forbidden by the inversion symmetry. Fig 4b shows the relative intensity of the SHG effect photo-induced as explained in subsection 2.3. Notice that a coherent bicolour IR optical treatment can be qualified as a specific ‘optical poling’, which breaks down the inversion symmetry of the crystal. For more detailed physical explanations of the effect we refer the reader to Refs. [27, 28] (see also Ref. [23] concerning extra features of the IR-induced second harmonics generation). Therefore we will discuss only the temperature dependence of the induced SHG shown in Fig. 4b. It is known (see [25]) that, as a rule, the most efficient ‘poling’ occurs in a vicinity of phase transitions. Therefore the temperatures between ~ 410 K (at heating) and ~ 400 K (at cooling) where the SHG effect reveals broad maximums (see Fig. 4b) might be suspected as an interval of some structural transformation. Then the thermal hysteresis of ~ 10 K would hint at a first-order character of this transformation.

As a matter of fact, a common feature of many ionic conductors, including the A_4BX_6 compounds, is a phase transition from a poorly conducting ordered low-temperature phase into highly conductive disordered high-temperature one. It happens, e.g., in the In_4CdI_6 crystals (see [17]). This polymorphic order-disorder transition can usually be characterised by a thermal hysteresis. However, the authors [17] have not found such a transition in Tl_4CdI_6, following from the conductivity data, and so have not regarded this material as an ionic conductor. Neither have they noticed a noticeable broadening of the Raman bands that might evidence structural disordering at high temperatures.

On the other hand, the authors [4] have stated availability of a phase transition in Tl_4CdI_6. In fact they have found a gently sloping minimum at ~ 400 K for the conductivity represented by Arrenius plot, as well as a small thermal hysteresis of the corresponding temperature dependence. Of course, the slope change appearing in the temperature dependence of their dielectric permittivity cannot be considered as a decisive factor while judging whether the phase transition really exists. In this relation, our photo-induced SHG data seem to be another experimental fact that favours an idea of phase transformation in Tl_4CdI_6. In respect to the points mentioned above, we are also to note that our preliminary results have testified a presence of a thermochromic transformation in Tl_4CdI_6 at about 400 K, which converts the visual colour of the crystal from grey green to yellow or orange. This also inclines us to suppose the existence of a phase transformation. As for our thermal expansion data, their sensitivity is perhaps not sufficient for disclosing relatively weak structural changes.

It is also instructive to mention a long-standing dispute concerning the ionic conductivity and the phase transition in the isomorphous Tl_4HgI_6. The authors [18] have argued that the compound does not reveal high enough ionic conductivity, though the studies [3, 5, 6] have reported the opposite. On the other hand, our recent studies of the thermal expansion, differential scanning calorimetry and the photo-induced SHG have suggested a phase transition in this compound. That is why the question of structural transformations in the A_4BX_6 compounds, including the crystals under study, could only be solved basing upon versatile experimental investigations. As a result, we summarise that the hypothesis of phase transformation in Tl_4CdI_6 put in this work still remains open.

4. Conclusion

In this work we have reported the results for the synthesis, growth and the initial structural and optical characterisations of a ternary halide Tl_4CdI_6. Utilisation of the Bridgman–Stockburger technique has yielded in single crystals of sufficiently high quality. Their X-structural studies have resulted in the lattice cell parameters very close to those found in the earlier works. Following from both the structural and the SHG experiments, we have demonstrated that Tl_4CdI_6 crystallises in the centrosymmetric tetragonal spatial symmetry group $P4/mnc$, again in compliance with the literature data. Our thermal expansion data testify that the lattice parameter along the c axis of Tl_4CdI_6 increases with increasing temperature, with the temperature slope descending almost linearly at higher temperatures.

Tl_4CdI_6 crystals are optically positive. Our optical characterisation has shown that Tl_4CdI_6 can be qualified as a wide-gap semiconductor. The crystal possesses a prominent optical anisotropy, which manifests itself as a large difference between the optical pseudogap values for the ordinary and extraordinary polarisations and the birefringence somewhat higher than 0.1. A combination of high transparency in the IR range, which represents a characteristic feature of ternary halides, and a large birefringence that should also be characteristic for this range (see, e.g., the data [9] for Tl_4HgI_6 crystals, which exhibit similar optical properties) should make Tl_4CdI_6 promising for different applications in the IR range.

Whereas our linear thermal expansion reveals no local temperature anomalies up to about 500 K, we have found a broad maximum in the temperature dependence of photo-induced SHG intensity in the region 400–410 K, which can be suspected as evidence of some structural transformation. Although the literature data on the subject are contradictory (see [4, 17]), we assume that this transformation, if really available, should be of a polymorphic type. Further highly sensitive experiments are needed in order to clear up a matter of thermal evolution of the structure and phase transformations in the Tl_4CdI_6 crystals. In particular, additional conductivity, differential scanning calorimetry and heat capacity measurements seem to be promising in this relation. The appropriate studies are now in progress.

References

1. Zandbergen H W, 1979. The crystal structure of α-thallium hexaiodochromate, α-Tl_4CrI_6. Acta Cryst. B. **35**: 2852–2855.
2. Ammlung R L, Scaringe R P, Ibers J A, Shriver D F and Whitmore D H, 1979. Trends in heavy-metal solid state ionic conductors: A comparison of Cu^+, Ag^+, In^+, and Tl^+ transport. J. Solid State Chem. **29**: 401–415.
3. Nagase H, Furukawa and Nakamura D, 1990. Electrical conductivity and thallium spin-lattice relaxation time measurements of Tl_4HgBr_6 and Tl_4HgI_6. Bull. Chem. Soc. Japan. **63**: 3329–3330.
4. Sreejith M Nair, Yahya A I, Rafiuddin and Afaq Ahmad, 1996. Ionic conductivity and dielectric constant of Tl_4CdI_6. Solid State Ionics. **86**–**88**: 137–139.
5. Sarfaraz Nawaz M and Rafiuddin, 2007. Ionic conduction and effect of cation doping in Tl_4HgI_6. Ionics. **13**: 35–40.
6. Kalyagin D S, Ermolenko Yu E and Vlasov Yu G, 2008. Diffusion of Tl-204 isotope and ionic conductivity in Tl_4HgI_6 membrane material for chemical sensors. Rus. J. Appl. Chem. **81**: 2172–2174.
7. Klintenberg M, Derenzo S E and Weber M J, 2002. Potential scintillators identified by electronic structure. Nucl. Instr. Meth. Phys. Res. A. **486**: 298–302.
8. Kahler D, Singh N B, Knuteson D J, Wagner B, Berghmans A, McLaughlin S, King M, Schwartz K, Suhre D and Gotlieb M, 2011. Performance of novel materials for radiation detection: Tl_3AsSe_3, $TlGaSe_2$, and Tl_4HgI_6. Nucl. Instr. Meth. Phys. Res. A. **652**: 183–185.
9. Avdienko K I, Badikov D V, Badikov V V, Chizhikov V I, Panyutin V L, Shevyrdyaeva G S, Shcherbakov S I and Shcherbakova E S, 2003. Optical properties of thallium mercury iodide. Opt. Mater. **23**: 569–573.
10. Singh N B, Suhre D R, Green K, Fernelius N and Hopkins F K, 2005. Periodically poled materials for long wavelength infrared (LWIR) NLO applications. J. Cryst. Growth. **274**: 132–137.
11. Hagemann B M and Weber B H-J, 1996. Are ternary halides useful materials for nonlinear optical applications? Appl. Phys. A. **63**: 67–74.
12. Von Berthold H J, Haas D and Tamme R, 1979. Die Kristallstruktur des Thallium(I)-hexaiodomercurat(II), Tl_4HgI_6. Zeit. anorg. allg. Chem. **456**: 29–40.
13. Beck H P and Milius W, 1988. ns^2 cations as a prerequisite for a structure type and their interaction in ternary halides with the formula type A_4BX_6 (A: In, Tl; B: Cd, Pb, Ge; X: Cl, Br, I). Zeit. anorg. allg. Chem. **652**: 105–114.
14. Tkachenko V I, Semrad E E, Traksler Z A and Kovach A P, 1990. Region of homogeneity of

Tl_4HgI_6. Izv. AN SSSR, Ser. Fiz. **26**: 2240–2242.

15. Huart J and Durif A, 1966. Structure de Tl_4HgI_6. Acad. Sci. C. R. Paris. **257**: 657–661.
16. Badikov D V, Badikov V V, Kuzmicheva G M, Panyutin V L, Rybakov V. B., Chizhikov V I, Shevyrdyaeva G S and Shcherbakova E S, 2004. Growth and X-ray diffraction study of Tl_4HgI_6 crystals. Inorganic Mater. **40**: 314–320.
17. Ammlung R L, Shriver D F, Kamimoto M and Whitmore D H, 1977. Conductivity and Raman spectroscopy of new indium(I) and thallium(I) ionic conductors. In_4CdI_6, In_2ZnI_4, Tl_2ZnI_4, and the related compound Tl_4HgI_6. J. Solid State Chem. **21**: 185–193.
18. Kennedy J H, Schaupp C, Yuan Yang and Zhengming Zhang, 1990. Composition and properties of thallium mercury iodide. J. Solid State Chem. **88**: 555–563.
19. Piasecki M, Lakshminarayana G, Fedorchuk A O, Kushnir O S, Franiv V A, Franiv A V, Myronchuk G and Plucinski K J, 2012. Temperature operated infrared nonlinear optical materials based on Tl_4HgI_6. J. Mater. Sci.: Mater. Electron. DOI: 10.1007/s10854-012-0903-6 (7 p.).
20. SRM 676: Alumina internal standard for quantitative analysis by X-ray powder diffraction (National Institute of Standards and Technology, US Department of Commerce) (Gaithersburg, MD, 2005).
21. Stoe WinX^{POW}. Version 3.03 (Darmstadt, Stoe & Cie GmbH, 2010).
22. Girnyk I S, Kushnir O S and Shopa R Y, 2005. Linear thermal expansion of ferroelectric deuterated triglycine sulphate. Ferroelectrics. **317**: 75–78.
23. Kityk I V, 2003. IR-induced second harmonic generation in Sb_2Te_3–BaF_2–$PbCl_2$ glasses. J. Phys. Chem. B. **107**: 10083–10087.
24. Balakirev M K, Smirnov V A, Vostrikova L I, Kityk I V, Kasperczyk J and Gruhn W, 2003. Giant increase of the second harmonic radiation's absorption during optical poling of oxide glass. J. Mod. Opt. **50**: 1237–1244.
25. Kassab L R P, de A Pinto R, Kobayashi R A, Piasecki M, Bragiel P and Kityk I V, 2007. Photoinduced non-linear optics of Eu_2O_3 doped TeO_2–GeO_2–PbO glasses. J. Phys. D: Appl. Phys. **40**: 1642–1645.
26. Shaskolskaya M P. Acoustic crystals. Moscow: Nauka (1982) (in Russian).
27. Zel'dovich B. Ya., Kapitskii Yu. E. and Churikov V M, 1991. Induced $\chi^{(2)}$ gratings in glasses. J. Exp. Theor. Phys. Lett. **53**: 78–81.
28. Dominic V and Feinberg J, 1993. Light-induced second-harmonic generation in glass via multiphoton ionization. Phys. Rev. Lett. **71**: 3446–3449.

Franiv A. V., Kushnir O. S., Girnyk I. S., Franiv V. A., Kityk I., Piasecki M. and Plucinski K. J. 2013. Growth, crystal structure, thermal properties and optical anisotropy of Tl_4CdI_6 single crystals. Ukr.J.Phys.Opt. 14: 6 – 14.

***Анотація**. Ми повідомляємо про вирощування та результати попередньої термічної та оптичної характеризації монокристалічного тернарного галоїду* Tl_4CdI_6*. За кімнатної температури кристали описуються центросиметричним тетрагональним класом P4/mnc. Вивчено параметри лінійного термічного розширення в діапазоні 330–500 К. Кристали оптично додатні і виявляють дуже високу оптичну анізотропію (подвійне заломлення ~ 0.13 при 633 нм). Величина їхньої оптичної псевдощілини відповідає широкозонним напівпровідникам. Широкий максимум при 400–410 К, знайдений у температурній залежності генерації другої гармоніки, індукованої ІЧ-випромінюванням, може вказувати на наявність поліморфного фазового перетворення.*